Journal of Molecular Graphics and Modelling 29 (2011) 591–596

Contents lists available at ScienceDirect

Journal of Molecular Graphics and Modelling

journal homepage: www.elsevier.com/locate/JMGM

How do carbon nanotubes serve as carriers for gemcitabine transport in a drug delivery system?

Uthumporn Arsawang[a], Oraphan Saengsawang[b,c], Thanyada Rungrotmongkol[b,c], Purinchaya Sornmee[a], Kitiyaporn Wittayanarakul[b,c,e], Tawun Remsungnen[d], Supot Hannongbua[b,c,*]

[a] Department of Mathematics, Faculty of Science, Chulalongkorn University, Bangkok 10330, Thailand
[b] Computational Chemistry Unit Cell, Department of Chemistry, Faculty of Science, Chulalongkorn University, Bangkok 10330, Thailand
[c] Center of Innovative Nanotechnology, Chulalongkorn University, Bangkok 10330, Thailand
[d] Department of Mathematics, Faculty of Science, Khon Kaen University, Khonkaen 40002, Thailand
[e] Program of Natural Resource and Environmental Management, School of Science and Technology, Khon Kaen University, Nongkhai Campus, Nongkhai 43000, Thailand

ARTICLE INFO

Article history:
Received 24 June 2010
Received in revised form 1 November 2010
Accepted 1 November 2010
Available online 11 November 2010

Keywords:
Carbon nanotube
Gemcitabine
Drug delivery
Molecular dynamics simulations
Steered molecular dynamics simulations

ABSTRACT

Aiming at understanding the molecular properties of the encapsulation of the anticancer drug gemcitabine in the single-walled carbon nanotube (SWCNT), molecular dynamics (MD) simulations were applied to the two scenarios; that of gemcitabine filling inside the SWCNT, and that of the drug in the free state. Inside the SWCNT, the cytosine ring of gemcitabine was found to form a π–π stacking conformation with the SWCNT surface, and this movement is not along the centerline of the tube from one end to the other of the tube where the distance from the center of gravity of the molecule to the surface is 4.7 Å. A tilted angle of 19° was detected between the cytosine ring of gemcitabine and the inner surface of SWCNT. In comparison to its conformation in the free form, no significant difference was observed on the torsion angle between the five- (ribose) and the six- (cytosine) membered rings. However, gemcitabine inside the SWCNT was found to have a lower number of solvating water molecules but with a stronger net solvation than the drug in the free state. This is due to the collaborative interactions between gemcitabine and the surface of the SWCNT. In addition, the steered molecular dynamics simulation (SMD) approach was employed to investigate the binding free energy for gemcitabine moving from one end to another end throughout the SWCNT. In excellent agreement with that yielded from the classical MD, the SMD energy profile confirms that the drug molecule prefers to locate inside the SWCNT.

1. Introduction

Since the discovery of carbon nanotubes (CNTs) in 1991 [1], they have been considered as the ideal material for a variety of applications owing to their unique properties. These properties include their potential biocompatibility in pharmaceutical drug delivery systems [2–4] and their excellent role as drug carriers with a highly site-selective delivery and sensitivity [5–10]. To accelerate the optimal development of CNT as a new effective drug transporter, it is required to better understand the structural properties of the drug–CNT complex.

As reported by the Centers for Disease Control and Prevention (CDC), cancer is the second leading cause in the number of deaths worldwide [11], and ovarian cancer, found in the female reproductive malignant cells [12], is the fifth most common cancer. Gemcitabine, in combination with carboplatin, is the main anticancer drug used to treat ovarian cancer [13]. Gemcitabine is a pro-drug, and as the active di- and tri-phosphate nucleosides, exhibits cell phase specificity, primarily killing cells undergoing DNA synthesis (S-phase) and also blocking the progression of cells through the G1/S-phase boundary. The cytotoxic effects of gemcitabine are exerted through incorporation of gemcitabine triphosphate (dFdCTP) into DNA, resulting in the inhibition of DNA synthesis and induction of apoptosis. However, this is not cancer cell specific and so the main problem, common to most cancer treatments and therapy, is the serious side effects to normal cells. Bone marrow toxicity is one such effect in patients who show adverse reactions to gemcitabine. To avoid such effects, the development of a drug delivery system to transport the drug molecules efficiently and specifically to the targeted tumor cells, without harming the surrounding tissue is one promising approach. This can lead to a more sustained and localized delivery of the drug, reducing the systemic loads and side effects to non-target cells. To this end CNTs have been found to show good carrier properties by serving as a

* Corresponding author at: Computational Chemistry Unit Cell, Department of Chemistry, Faculty of Science, Chulalongkorn University, Bangkok 10330, Thailand. Tel.: +66 22 187602; fax: +66 22 187603.
E-mail address: supot.h@chula.ac.th (S. Hannongbua).

1093-3263/$ – see front matter © 2010 Elsevier Inc. All rights reserved.
doi:10.1016/j.jmgm.2010.11.002

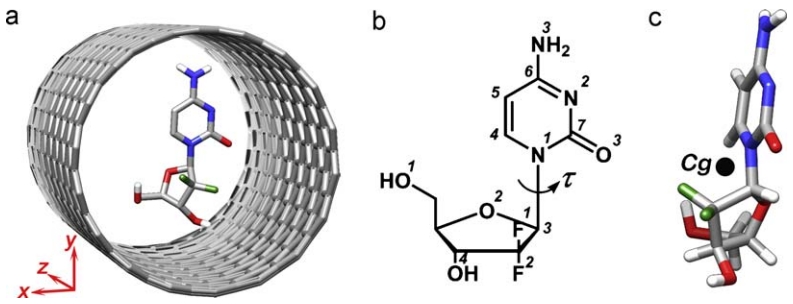

Fig. 1. (a) The structure of the (18,0) single-walled carbon nanotube (SWCNT) complexed with the gemcitabine drug. (b) The atomic labels and torsion angle, τ, of drug are defined. The origin of the Cartesian coordinate for the complex was centered at the center of gravity (*Cg*) of the SWCNT where (c) the *Cg* position of drug molecule is also shown.

transporter of bio-molecules to the target site of a diverse array of compounds, including drugs [14–18], vaccines [19,20], small peptides [21,22], proteins [23–26], nucleic acids [27–30], vitamins and sugars [31,32]. Basically, these molecules are attached on either the inner or outer tube wall surfaces, which are the so-called filling or wrapping modes of binding, respectively. Functionalized CNTs were also proposed as promising materials as they were found to reduce the toxic nature of the pristine (non-functionalized) CNT in both *in vitro* and *in vivo* applications [33–35].

The present study aims to examine the structure, orientation, conformation, solvation and movement of the anticancer drug gemcitabine inside a pristine zigzag (18,0) single-walled carbon nanotube (SWCNT) in aqueous solution using a molecular dynamics simulation approach. The properties of gemcitabine in the free form (without SWCNT bound) in aqueous solution were also studied and compared. In addition, the steered molecular dynamics simulation (SMD) [36] was applied to examine the binding free energy profile when gemcitabine moves, from one end to another end, throughout the SWCNT.

2. Model and method

2.1. Preparation of the starting structures

Zigzag (18,0) SWCNT with a diameter of 14 Å was used as the model carrier to examine the gemcitabine–SWCNT drug carrier. The SWCNT structure was generated from the Nanotube Modeler package [37] with chiral vectors $m = 18$, $n = 0$ and 34 Å in length (Fig. 1a). The molecular dynamics simulations were carried out for two systems; free gemcitabine and its complex with SWCNT, both solvated in an aqueous solution.

To construct the molecular geometry of the gemcitabine–SWCNT complex, the crystal structure of gemcitabine bound to human deoxycytidine kinase (Protein Data Bank (PDB) [38], code 2NO0) was used to excise the gemcitabine structure and this was then placed in the middle of the pore of a pristine SWCNT (Fig. 1a). Hydrogen atoms were added to the drug molecule and both ends of the tube using the LEaP module in the AMBER 9 software package [39].

The parameters of the SWCNT were taken from the AMBER 99 force field [40] where the atom type CA was chosen to represent the aromatic carbon atoms. A general comment on the applicability of this force field to CNT can be found elsewhere [41,42]. For the gemcitabine molecule, the parameters for the 5- and 6- membered rings were, respectively, created by considering those of the ribose and cytosine, while the parameters involving the fluorine atoms were generated from the Generalized AMBER Force Field (GAFF) [40]. To obtain the atomic charges of gemcitabine, the following procedures were carried out. Firstly, the molecular structure of the gemcitabine was fully optimized using the Gaussian03 program [43] at the Hartree-Fock level of theory using the 6-31G* basis set. Then, the electrostatic potentials (ESP) surrounding the compound were computed at the same basis set and level of theory. The RESP charge-fitting procedure was applied and the partial charges of equivalent atoms were fitted into the identical value using the RESP module of AMBER 9.

The drug in free state and the drug–SWCNT complex were both solvated with a SPC/E [44] octagonal box over 12 Å from the system surface. Any water molecules in which the oxygen atoms sterically overlapped with the heavy atoms of the drug and the SWCNT molecules were removed. Here, the systems of the free drug and its complex with SWCNT contain 3296 and 14627 atoms in total, respectively.

2.2. Classical molecular dynamics (MD) simulations

The simulations were performed using the SANDER module in the AMBER 9 program package with the *NPT* ensemble at 1 atm and a time step of 2 fs. The SHAKE algorithm [45] was applied to all bonds involving hydrogen atoms to constrain their motions. The periodic boundary conditions were applied and the cutoff function was set at 12 Å for nonbonded interactions and particle mesh Ewald method [46,47]. The whole system was heated from 100 K to 300 K for 25 ps and equilibrated at 300 K for 600 ps. Then, the production stage was performed for 10 ns in which the structural coordinates were saved every 1 ps for analysis.

2.3. Steered molecular dynamics (SMD) simulations

Basic concept of the SMD technique [36] is to apply the external forces to particles in a selected direction by employing a harmonic (spring-like) restraint to the system in order to create greater change of the particle coordinates, relative to classical MD. In this study, the gemcitabine was generated to locate at 25 Å far from one end of the SWCNT on the vector which pointing through the *Cg* of the SWCNT and parallel to the tube axis. The external forces were then employed to all drug atoms in the direction along the selected vector. The pulling atoms were harmonically constrained with a force $F = -k(x - vt)$, where k, x, v and t are the spring constant, atom coordinates, atom velocities, and integration time step, respectively [48,49]. The value of k was set to $7k_BT/Å^2$, which relates to a thermal fluctuation of the pulling atoms of 0.38 Å, $(k_BT/k)^{1/2}$ where T denotes temperature in Kelvin and k_B is Boltzman's constant [48,49]. A dielectric constant of 1 and an integration time step of 2 fs were set throughout the SMD simulation. Switching distance required for smoothing between electrostatic and van der Waals interactions is within the range 10–12 Å. With the applied velocity of 0.0035 Å ps^{-1}, drug was found to exit the SWCNT at 600 ps.

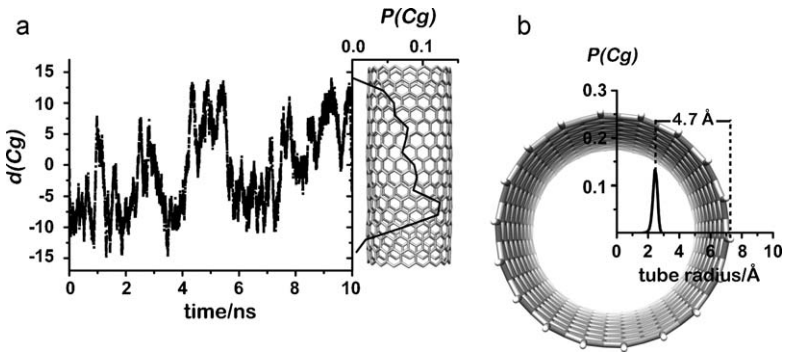

Fig. 2. (a) Displacement of the center of gravity of gemcitabine, $d(Cg)$, as a function of the simulation time (horizontal plot), and the probability of finding the gemcitabine Cg (vertical plot), $P(Cg)$, projected onto the SWCNT z-axis. (b) The $P(Cg)$ in directions perpendicular to the SWCNT surface (x- and y-axis).

Note that, the other atoms in the system, including the explicit water molecules, were treated by the classical MD approach. The coordinates of system were collected every 0.2 ps.

3. Results and discussion

3.1. Localization of gemcitabine within the drug–SWCNT complex

To examine the feasibility of using SWCNT as a nano-container for gemcitabine delivery applications, the drug–SWCNT complex was monitored in terms of the gemcitabine center of gravity (Cg) distribution inside the SWCNT. Along the SWCNT's axis (z-axis defined in Fig. 1a), the displacement of the gemcitabine Cg, $d(Cg)$, as a function of simulation time is shown in the horizontal plot in Fig. 2a, while the probability of finding the gemcitabine Cg, $P(Cg)$, is illustrated in the vertical plot of the same figure. To monitor the movement of the drug in the direction perpendicular to the SWCNT surface, the averaged projection of the $P(Cg)$ to the tube x- and y-axis (defined in Fig. 1a) were also calculated, and are shown in Fig. 2b.

In Fig. 2a, the $d(Cg)$ in the horizontal plot shows that at the initial step ($t = 0$), the gemcitabine was located at the center of the SWCNT ($Cg = 0$). Regular movement of the drug molecule from one end ($d(Cg) = -12.5$ Å) to the other ($d(Cg) = +12.5$ Å) of the 34 Å SWCNT can be clearly seen. In addition, gemcitabine was never found at the inner surface at a distance of <4.5 Å from the two ends of the tube, *i.e.*, the gemcitabine is able to move freely and remain only inside its container. This is likely due to breaking the π–π interactions between the cytosine group and the tube wall at the ends. The observed event was well supported by the $P(Cg)$ plot (the vertical plot in Fig. 2a), where the probability was found to increase exponentially as a function of the distance from the two ends of the SWCNT. Note that a symmetric distribution of the $P(Cg)$ plot is expected if the sampling size is large enough, with a long enough simulation time.

In the same manner, the probability of finding the gemcitabine Cg in the direction perpendicular to the tube surface (x- and y-axis) showed only one distinct peak at 2.3 Å from the origin of the coordinate system, indicating that gemcitabine does not prefer to move at the center along the tube z-axis but rather that the favorite motion is ~4.7 Å away from the inner surface instead. It is, therefore, likely that an aromatic stacking interaction between the gemcitabine and the SWCNT surface was formed (discussed in the next section). Taking into account all the above mobility data, gemcitabine was found to coordinate inside the SWCNT, forming the drug–SWCNT complex, during the whole simulation time of 10 ns. Therefore, the SWCNT terminated by the hydrogen atoms is assumed to be suitable as a drug container for a gemcitabine delivery system.

3.2. Conformation of gemcitabine in the free and SWCNT-complexed forms

To examine the conformation as well as the flexibility of gemcitabine in the free state and that when inside the SWCNT, the relative orientation of the ribose ring (five-membered ring) and cytosine ring (six-membered ring), defined as the C^7–N^1–C^3–O^2 torsion angle (τ) in Fig. 1b, was calculated and compared. No significant difference was found between the gemcitabine conformations in these two states (Fig. 3), where the most probable torsion angle of the free and SWCNT-complexed forms was observed at 210° and 215°, respectively. Note that the distribution plot showed a broad peak covering the range of 80°, precisely from 170° to 250° for the free form and from 180° to 260° for the complex. This suggested that the drug molecule is rather flexible and insensitive to the environment, both when free in the aqueous solution and when complexed inside the SWCNT. Therefore, utilizing CNT as the gemcitabine carrier does not affect the conformation of the drug itself and so, presumably, does not affect its stability and bioactivity.

To understand more details of the molecular alignment of gemcitabine inside the SWCNT, the atom–atom radial distribution functions (RDFs), expressed as $g_{ij}(r)$ the probability of finding a particle of type j in a sphere of radius, r, around a particle of type i, were calculated. Interest here was focused onto the cytosine (six-membered) ring whose π-aromatic system was expected to preferably be deposited and to directly interact with the inner surface of the SWCNT. Therefore, in this study i denotes the backbone atoms of the cytosine ring (C^4–C^7, N^1 and N^2) and j represents the carbon atoms of the SWCNT. The calculated RDFs are summarized in Fig. 4a, whilst a schematic representation of the drug–SWCNT complex, where vector $\vec{a}$ lies parallel to the SWCNT surface and vector $\vec{b}$ points from C^6 to N^1 atoms, is shown in Fig. 4b.

The six RDF plots (Fig. 4a) can be classified into three sets, {C^5, C^6, N^2}, {C^4, C^7} and {N^1}, in which their $g(r)$s were detected for the first time ($g(r) \neq 0$) at 3.0 Å, 3.4 Å and 3.8 Å with the maxima

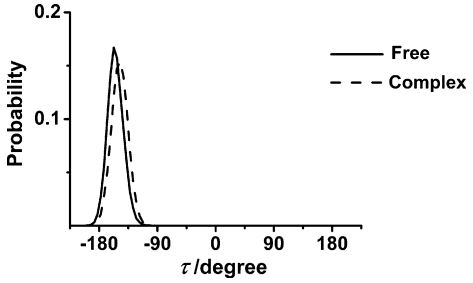

Fig. 3. Distribution of the C^7–N^1–C^3–O^2 torsion angle, τ (see Fig. 1b for its definition and atomic labels), of the gemcitabine in the free (solid line) and SWCNT-complexed (dash line) forms.

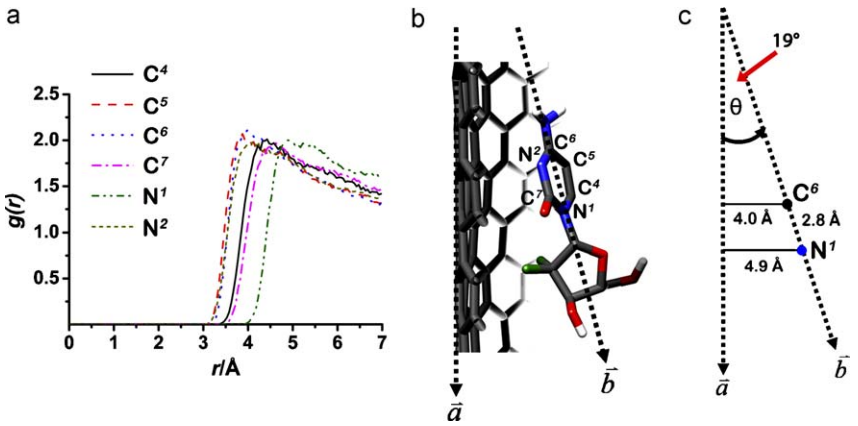

Fig. 4. (a) RDFs centered at the atoms in the cytosine (six-membered) ring of the gemcitabine drug (C^4–C^7, N^1 and N^2) to the carbon atoms of the SWCNT. (b) Schematic representation of the gemcitabine–SWCNT complex where vector $\vec{a}$ lies parallel to the SWCNT surface and vector $\vec{b}$ points from the C^6 to the N^1 atoms. (c) Estimated angle between vectors $\vec{a}$ and $\vec{b}$ (see text for details of the related distances).

at ~4.0 Å, ~4.5 Å and 4.9 Å, respectively. Using the most probable distances from the C^6 (~4.0 Å maximum of the C^6–C RDF) and N^1 (~4.9 Å maximum of the N^1–C RDF) atoms to the SWCNT surface, and the N^1–C^6 distance (2.8 Å), the angle between the vectors $\vec{a}$ and $\vec{b}$ can be estimated (Fig. 4c). The obtained value of 19° indicates the tilted angle representing the configuration of the π–π stacking interaction between the cytosine ring of the gemcitabine and the inner surface of the SWCNT. This interaction is supposed to be the main reason why the preferential mobility of the drug molecule along the molecular *z*-axis of the SWCNT takes place at ~4.7 Å far from the surface of the SWCNT (Fig. 2b).

3.3. Solvation of gemcitabine in free solution and complexed with SWCNT

The ligand solvation was monitored by the atom–atom radial distribution functions. Here, the RDFs to the oxygen atom of water around the heteroatom in the gemcitabine were evaluated and plotted in Fig. 5 for gemcitabine in both the free solvated and SWCNT-complexed forms. The corresponding running integration numbers, $n(r)$, were also calculated and are shown. The first shell coordination number, *CN*, around the atoms of drug (defined in Fig. 1b) in both systems, which were obtained from the integration up to the first minimum of the RDF, are summarized in Table 1.

The plots for both systems showed almost sharp first peaks, indicating a strong solvation and high water accessibility, to the central atoms of the drug molecule. Among all oxygens, the O^2 atom is much less accessible than the others owing to the steric hindrance to solvation in 5-membered ring. Remarkable changes were found on the RDFs of the fluorine atoms, especially F^1. In the complex form, the first shell RDF of F^2 atom displayed the lower intensity while that of F^1 atom was almost disappeared; *i.e.*, water molecules cannot feasibly gain access to these two atoms. This is due to the fact that these gemcitabine atoms in the SWCNT-complexed form were turned to approach to the SWCNT surface (see Fig. 4b). Moreover, a considerable difference was also observed in the height of the $g(r)$ in the region between the first and the second peaks of almost all RDFs, which denotes the feasibility of water exchange between the two shells. These values for the drug in the free form (Fig. 5a, c, and e) were noticeably higher than those in the SWCNT-complexed forms, which imply that water molecules in the first hydration shell bind stronger to the drug atoms in the complex form than those in the free form. The likely reason for this finding is because of the col-

Table 1
First shell coordination number, *CN*, around the atoms of gemcitabine in the free and SWCNT-complexed forms, obtained from the integration up to the first minimum of the atom-atom RDF, $g(r)$, shown in Fig. 5.

Atom	CN	
	Free	Complex
O^1	2.5	2.4
O^2	0.7	0.6
O^3	3.0	2.3
O^4	2.6	2.5
N^1	–	0.8
N^2	1.5	1.0
N^3	3.8	3.3
F^1	4.7	–
F^2	6.5	2.3

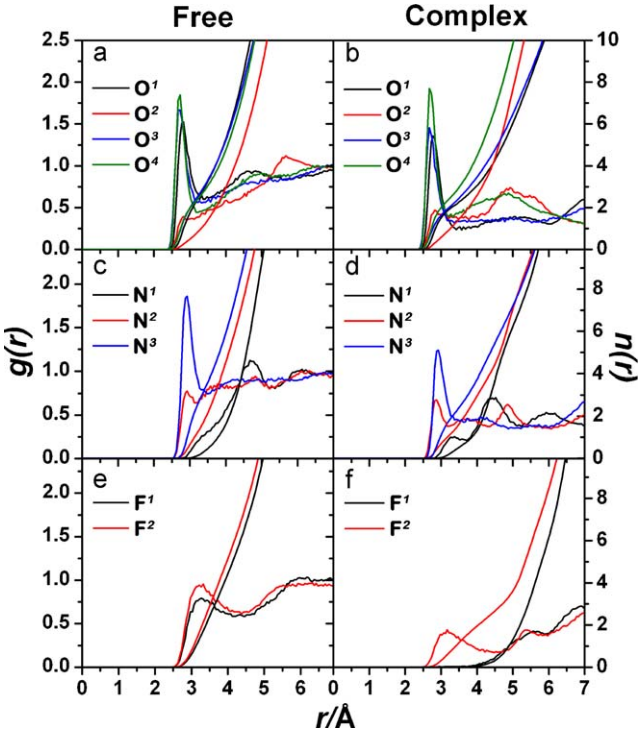

Fig. 5. Radial distribution functions, $g(r)$, centered on the inhibitor atoms (see Fig. 1b for atomic labels) to the oxygen atoms of the modeled water for gemcitabine in the free and SWCNT-complexed systems, including the running integration number up, $n(r)$.

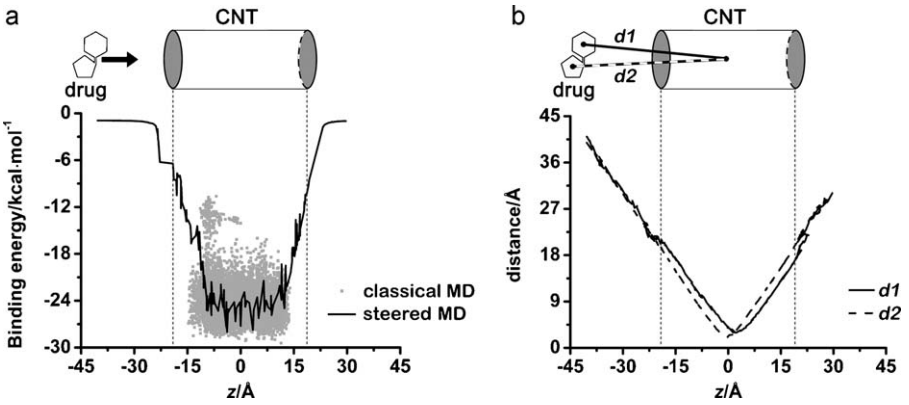

Fig. 6. (a) Binding free energies between the SWCNT and the gemcitabine drug obtained from the classical and the steered MD simulations, and (b) the d1 and d2 distances (defined in the inset) from *Cg* of the SWCNT to *Cgs* of the six- (cytosine) and five- (ribose) of drug molecule, respectively, as a function of the distance along tube (*z*) axis.

laborative effect due to the aromatic stacking interactions with the inner surface of the SWCNT (see also Fig. 4b), as discussed above.

Changes in the first shell coordination numbers of gemcitabine, in comparison between its free and SWCNT-complexed states (Table 1), can be classified into three sets; notably a marked decrease $\{F^1, F^2\}$, a slightly decreased $\{O^3, N^1, N^2, N^3\}$ and lastly those that were almost the same $\{O^1, O^2, O^4\}$. This is a consequence of the conformational changes of gemcitabine, where the three sets of atoms in the complexed form were located in the following three configurations relative to the SWCNT surface (Fig. 4b); (i) $\{F^1, F^2\}$ was tabbed between the SWCNT inner surface and the five-membered ring (almost no space is available for the solvent); (ii) $\{O^3, N^1, N^2, N^3\}$ were positioned in the plane of the six-membered ring that is coordinated in the stacked conformation to the SWCNT surface (only half of the space around the atoms can be solvated); and (iii) $\{O^1, O^2, O^4\}$ was tilted to point away from the SWCNT surface and the atoms in the SWCNT–gemcitabine complex are fully solvated, the same as that found as in the free form.

3.4. Binding free energy profile via the movement through the SWCNT

To examine characteristics of the gemcitabine's movement from one end to another end throughout the tube, binding free energy profile from the steered MD simulations was evaluated using the MM/PBSA procedure successfully applied in our previous works [50–52]. The results were given in Fig. 6a in comparison with those yielded from the classical MD. To monitor drug's conformation along the steered MD energy profile, the two distances d1 and d2 measured from *Cgs* of the six- (cytosine) and five- (ribose) rings of drug to *Cg* of the SWCNT were, respectively, defined in an inset in Fig. 6b. Changes of those distances as a function of the tube axis (*z*-axis) were calculated and shown in the same figure.

As expected, the SMD binding free energy (solid line in Fig. 6a) is almost zero when gemcitabine locates outside ($-40\,\text{Å} \le z \le -27\,\text{Å}$), and decreases rapidly after the molecule enters the SWCNT ($-15\,\text{Å} \le z \le -10\,\text{Å}$). The energy remains constant with the average of about -25 kcal mol^{-1} in the range $-10\,\text{Å} \le z \le 10\,\text{Å}$ and increase again afterward. This is in excellent agreement with that yielded from the classical MD (grey dot in Fig. 6a) when the drug molecule moves within the SWCNT. The two independent sources of energy data indicate clearly that drug molecule prefers to locate inside the SWCNT with a rather high energy barrier of -25 kcal mol^{-1} to exit from the tube. In terms of the drug's conformation, d1 (defined in an inset) is about 3.82 Å longer than d2 at $z < 0$ Å (Fig. 6b) and in *vice versa*. This indicates evidently that the ribose ring of gemcitabine points to enter into one end and exit from another end of the tube.

4. Conclusions

MD simulations provide insight into the structural properties of SWCNT serving as a gemcitabine drug carrier. The conformation, orientation and solvation of gemcitabine, as well as its movement inside the SWCNT, was extensively investigated in comparison to those of the drug in the free solvated state. According to the local density distributions of the drug projected to the diameter (*xy*-plane) and the length (*z*-axis) of the SWCNT, gemcitabine was able to simultaneously translocate from one end to the other of the SWCNT. This movement is not along the centerline of the tube, but rather the displacement is at a distance from the *C*(*g*) of gemcitabine of 4.7 Å from the inner surface of the tube, where the cytosine ring of gemcitabine is oriented with a 19° tilted angle to the SWCNT inner surface. This information indicates that the drug molecule always exists inside the tube and is in the π–π stacking conformation between its cytosine ring and the tube surface. Although, the relative conformations between the cytosine and ribose rings in both the free and SWCNT-complexed states were almost identical, the loss of drug solvation around the drug molecule, especially the F^1 and F^2 atoms, were found in the drug–SWCNT complex. This is a result of the collaborative interaction with the surface of the tube. In addition, the binding free energy profile of the gemcitabine via its movement from outside through the SWCNT was also investigated using steered MD. The result is in good agreement with that obtained from the classical MD, *i.e.*, drug molecule prefers to locate inside the SWCNT.

Acknowledgments

This work was supported by The Thailand Research Fund (TRF), and the Thai Government Stimulus Package 2 (TKK2555), under the Project for Establishment of Comprehensive Center for Innovative Food, Health Products and Agriculture. U.A. would like to acknowledge the M.Sc. program from the Development and Promotion of Science and Technology Talents project (DPST) and the graduate school Chulalongkorn University. O.S. thanks the Commission on Higher Education, and T.R. and K.W. thank the Ratchadaphiseksomphot Endowment Fund from Chulalongkorn University for the Post Doctoral Program. T.R. also thanks the TRF Grant for New Research (Grant No. TRG5280035). The HPC service at National Electronics and Computer Technology Center (NECTEC) and the Applied Mathematics Research Group (AMRG) at Khon Kaen University provided the computing facilities. The Center of Excellence for Petroleum, Petrochemicals and Advanced Materials, Chulalongkorn University, is acknowledged.

References

[1] S. Iijima, Helical microtubules of graphitic carbon, Nature 354 (1991) 56–58.
[2] A. Bianco, K. Kostarelos, C.D. Partidos, M. Prato, Biomedical applications of functionalised carbon nanotubes, Chem. Commun. (2005) 571–577.
[3] S.K. Smart, A.I. Cassady, G.Q. Lu, D.J. Martin, The biocompatibility of carbon nanotubes, Carbon 44 (2006) 1034–1047.
[4] A.M. Popov, Y.E. Lozovik, S. Fiorito, L.H. Yahia, Biocompatibility and applications of carbon nanotubes in medical nanorobots, Int. J. Nanomed. 2 (2007) 361–372.
[5] S. Banerjee, T. Hemraj-Benny, S.S. Wong, Covalent surface chemistry of single-walled carbon nanotubes, Adv. Mater. 17 (2005) 17–29.
[6] G. Pastorin, W. Wu, S.B. Wieckowski, J.-P. Briand, K. Kostarelos, M. Prato, et al., Double functionalisation of carbon nanotubes for multimodal drug delivery, Chem. Commun. (2006) 1182–1184.
[7] C. Klumpp, K. Kostarelos, M. Prato, A. Bianco, Functionalized carbon nanotubes as emerging nanovectors for the delivery of therapeutics, Biochim. Biophys. Acta: Biomembr. 1758 (2006) 404–412.
[8] K. Kostarelos, L. Lacerda, G. Pastorin, W. Wu, J. WieckowskiSebastien, Luangsivilay, et al., Cellular uptake of functionalized carbon nanotubes is independent of functional group and cell type, Nat. Nanotechnol. 2 (2007) 108–113.
[9] V. Raffa, G. Ciofani, S. Nitodas, T. Karachalios, D. D'Alessandro, M. Masini, et al., Can the properties of carbon nanotubes influence their internalization by living cells? Carbon 46 (2008) 1600–1610.
[10] X. Zhang, L. Meng, Q. Lu, Z. Fei, P.J. Dyson, Targeted delivery and controlled release of doxorubicin to cancer cells using modified single wall carbon nanotubes, Biomaterials 30 (2009) 6041–6047.
[11] http://www.cdc.gov/nchs/FASTATS/deaths.htm.
[12] http://www.reuters.com/article/idUKN1930660220080220.
[13] M.F. Kose, M.M. Meydanli, G. Tulunay, Gemcitabine plus carboplatin in platinum-sensitive recurrent ovarian carcinoma, Expert Rev. Anticancer Ther. 6 (2006) 437–443.
[14] A. Bianco, K. Kostarelos, M. Prato, Applications of carbon nanotubes in drug delivery, Curr. Opin. Chem. Biol. 9 (2005) 674–679.
[15] R.P. Feazell, N. Nakayama-Ratchford, H. Dai, S.J. Lippard, Soluble single-walled carbon nanotubes as longboat delivery systems for platinum (IV) anticancer drug design, J. Am. Chem. Soc. 129 (2007) 8438–8439.
[16] Z. Liu, X.M. Sun, N. Nakayama-Ratchford, H.J. Dai, Supramolecular chemistry on water-soluble carbon nanotubes for drug loading and delivery, ACS Nano 1 (2007) 50–56.
[17] Z. Liu, K. Chen, C. Davis, S. Sherlock, Q.Z. Cao, X.Y. Chen, et al., Drug delivery with carbon nanotubes for *in vivo* cancer treatment, Cancer Res. 68 (2008) 6652–6660.
[18] C. Srinivasan, Carbon nanotubes in cancer therapy, Curr. Sci. 94 (2008) 300–301.
[19] A. Bianco, M. Prato, Can carbon nanotubes be considered useful tools for biological applications? Adv. Mater. 15 (2003) 1765–1768.
[20] C. Salvador-Morales, E. Flahaut, E. Sim, J. Sloan, M.L.H. Green, R.B. Sim, Complement activation and protein adsorption by carbon nanotubes, Mol. Immun. 43 (2006) 193–201.
[21] D. Pantarotto, C.D. Partidos, R. Graff, J. Hoebeke, J.-P. Briand, M. Prato, et al., Synthesis, structural characterization, and immunological properties of carbon nanotubes functionalized with peptides, J. Am. Chem. Soc. 125 (2003) 6160–6164.
[22] D. Pantarotto, C.D. Partidos, J. Hoebeke, F. Brown, E. Kramer, J.-P. Briand, et al., Immunization with peptide-functionalized carbon nanotubes enhances virus-specific neutralizing antibody responses, Chem. Biol. 10 (2003) 961–966.
[23] D. Pantarotto, J.-P. Briand, M. Prato, A. Brianco, Translocation of bioactive peptides across cell membranes by carbon nanotubes, Chem. Commun. (2004) 16–17.
[24] N.W.S. Kam, H. Dai, Carbon nanotubes as intracellular protein transporters: generality and biological functionality, J. Am. Chem. Soc. 127 (2005) 6021–6026.
[25] K. Yanagi, K. Iakoubovskii, S. Kazaoui, N. Minami, Y. Maniwa, Y. Miyata, et al., Light-harvesting function of beta-carotene inside carbon nanotubes, Phys. Rev. B 74 (2006) 155420.
[26] K. Yanagi, Y. Miyata, H. Kataura, Highly stabilized β-carotene in carbon nanotubes, Adv. Mater. 18 (2006) 437–441.
[27] H. Gao, Y. Kong, D. Cui, C.S. Ozkan, Spontaneous insertion of DNA oligonucleotides into carbon nanotubes, Nano Lett. 3 (2003) 471–473.
[28] N.W.S. Kam, Z. Liu, H. Dai, Functionalization of carbon nanotubes via cleavable disulfide bonds for efficient intracellular delivery of siRNA and potent gene silencing, J. Am. Chem. Soc. 127 (2005) 12492–12493.
[29] Y. Liu, D.-C. Wu, W.-D. Zhang, X. Jiang, C.-B. He, T.S. Chung, et al., Polyethylenimine-grafted multiwalled carbon nanotubes for secure noncovalent immobilization and efficient delivery of DNA, Angew. Chem. Int. Ed. 44 (2005) 4782–4785.
[30] Z. Liu, M. Winters, M. Holodniy, H.J. Dai, siRNA delivery into human T cells and primary cells with carbon-nanotube transporters, Angew. Chem. Int. Ed. 46 (2007) 2023–2027.
[31] Y.H. Xie, A.K. Soh, Investigation of non-covalent association of single-walled carbon nanotube with amylose by molecular dynamics simulation, Mater. Lett. 59 (2005) 971–975.
[32] J. Xie, Q. Xue, Q. Zheng, H. Chen, Investigation of the interactions between molecules of [beta]-carotene, vitamin A and CNTs by MD simulations, Mater. Lett. 63 (2009) 319–321.
[33] V.L. Colvin, The potential environmental impact of engineered nanomaterials, Nat. Biotechnol. 21 (2003) 1166–1170.
[34] C.M. Sayes, F. Liang, J.L. Hudson, J. Mendez, W. Guo, J.M. Beach, et al., Functionalization density dependence of single-walled carbon nanotubes cytotoxicity *in vitro*, Toxicol. Lett. 161 (2006) 135–142.
[35] M. Prato, K. Kostarelos, A. Bianco, Functionalized carbon nanotubes in drug design and discovery, Acc. Chem. Res. 41 (2007) 60–68.
[36] M. Gao, M. Wilmanns, K. Schulten, Steered molecular dynamics studies of titin II domain unfolding, Biophys. J. 83 (2002) 3435–3445.
[37] http://www.jcrystal.com/products/wincnt/, Nanotube Modeler, JCrystalSoft Ed., 2004–2005.
[38] http://www.drugbank.ca/.
[39] D.A. Case, T.A. Darden, I.T.E. Cheatham, C.L. Simmerling, J. Wang, R.E. Duke, et al., AMBER 10, U.O. California Ed., San Francisco, 2008.
[40] J. Wang, R.M. Wolf, J.W. Caldwell, P.A. Kollman, D.A. Case, Development and testing of a general amber force field, J. Comput. Chem. 25 (2004) 1157–1174.
[41] Y. Cheng, D. Li, B. Ji, X. Shi, H. Gao, Structure-based design of carbon nanotubes as HIV-1 protease inhibitors: atomistic and coarse-grained simulations, J. Mol. Graphics Modell. 29 (2010) 171–177.
[42] C. Wei, Adhesion and reinforcement in carbon nanotube polymer composite, Appl. Phys. Lett. 88 (2006) 093108-1–093108-3.
[43] M.J.T. Frisch, G.W. Trucks, H.B. Schlegel, G.E. Scuseria, M.A. Robb, J.R. Cheeseman Jr., J.A. Montgomery, T. Vreven, K.N. Kudin, J.C. Burant, J.M. Millam, S.S. Iyengar, J. Tomasi, V. Barone, B. Mennucci, M. Cossi, G. Scalmani, N. Rega, G.A. Petersson, H. Nakatsuji, M. Hada, M. Ehara, K. Toyota, R. Fukuda, J. Hasegawa, M. Ishida, T. Nakajima, Y. Honda, O. Kitao, H. Nakai, M. Klene, X. Li, J.E. Knox, H.P. Hratchian, J.B. Cross, V. Bakken, C. Adamo, J. Jaramillo, R. Gomperts, R.E. Stratmann, O. Yazyev, A.J. Austin, R. Cammi, C. Pomelli, J.W. Ochterski, P.Y. Ayala, K. Morokuma, G.A. Voth, P. Salvador, J.J. Dannenberg, V.G. Zakrzewski, S. Dapprich, A.D. Daniels, M.C. Strain, O. Farkas, D.K. Malick, A.D. Rabuck, K. Raghavachari, P. Foresman, I. Komaromi, R.L. Martin, D.J. Fox, T. Keith, M.A. Al-Laham, C.Y. Peng, A. Nanayakkara, M. Challacombe, P.M.W. Gill, B. Johnson, W. Chen, M.W. Wong, C. Gonzalez, J.A. Pople, Gaussian 03 Revision C. 02, Gaussian Inc., Wallingford, CT, 2004.
[44] H.J.C. Berendsen, J.R. Grigera, T.P. Straatsma, The missing term in effective pair potentials, J. Phys. Chem. 91 (1987) 6269–6271.
[45] S. Miyamoto, P.A. Kollman, Settle: an analytical version of the SHAKE and RATTLE algorithm for rigid water models, J. Comput. Chem. 13 (1992) 952–962.
[46] T. Darden, D. York, L. Pedersen, Particle mesh Ewald: an N [center-dot] log(N) method for Ewald sums in large systems, J. Chem. Phys. 98 (1993) 10089–10092.
[47] U. Essmann, L. Perera, M.L. Berkowitz, T. Darden, H. Lee, L.G. Pedersen, A smooth particle mesh Ewald method, J. Chem. Phys. 103 (1995) 8577–8593.
[48] J.C. Phillips, R. Braun, W. Wang, J. Gumbart, E. Tajkhorshid, E. Villa, et al., Scalable molecular dynamics with NAMD, J. Comput. Chem. 26 (2005) 1781–1802.
[49] S. Kumar, C. Huang, G. Zheng, E. Bohm, A. Bhatele, J.C. Phillips, et al., Scalable molecular dynamics with NAMD on the IBM Blue Gene/L system, IBM J. Res. Dev. 52 (2008) 177–188.
[50] T. Rungrotmongkol, N. Nunthaboot, M. Malaisree, N. Kaiyawet, P. Yotmanee, A. Meeprasert, et al., Molecular insight into the specific binding of ADP-ribose to the nsP3 macro domains of chikungunya and venezuelan equine encephalitis viruses: molecular dynamics simulations and free energy calculations, J. Mol. Graphics Modell. (2010), doi:10.1016/j.jmgm.2010.09.2010.
[51] O Aruksakunwong, M. Malaisree, P. Decha, P. Sompornpisut, V. Parasuk, S. Pianwanit, et al., On the lower susceptibility of oseltamivir to influenza neuraminidase subtype N1 than those in N2 and N9, Biophys. J. 92 (2007) 798–807.
[52] M. Malaisree, T. Rungrotmongkol, P. Decha, P. Intharathep, O. Aruksakunwong, S. Hannongbua, Understanding of known drug-target interactions in the catalytic pocket of neuraminidase subtype N1, Proteins 71 (2008) 1908–1918.